Indian Journal of Chemical Technology
Vol. 27, January, 2020, pp. 51-59

Adsorption of cationic dye methyl green from aqueous solution onto activated carbon prepared from *BrachychitonPopulneus* fruit shell

Kamel Rida*, Keltoum Chaibeddra & Khadjidja Cheraitia

Laboratoire d'Interactions Matériaux et Environnement (LIME)Université Mohamed SeddikBenYahia-Jijel (Algeria)

E-mail: rida_kamel2001@yahoo.fr

Received 5 September 2018; accepted 30 May 2019

Activated carbon adsorbent prepared from *Brachychiton Populneus* fruit shell, biomass materials, is used for the removal of Methyl Green (MG) from aqueous solutions. For the purposes of the experiment (characterization of the adsorbent), we have used various methods, namely BET, FTIR and SEM. The various parameters influencing adsorption: contact time, initial concentration, mass of the adsorbent and temperature have been studied in batch systems. The modeling of the experimental data showed that the pseudo-second order model perfectly described the adsorption kinetics and the Langmuir model seems to be the most suitable for the equilibrium data with a maximum adsorption capacity of 67.93 mg/g. The thermodynamic study revealed that the adsorption of the MG dye is a spontaneous and exothermic phenomenon. This study confirms that activated carbon prepared from agricultural wastes has a high adsorption potential, making it an effective means for removing MG from aqueous solutions.

Keywords: Activated carbon, Biomass materials, Methyl green, Kinetics, Isotherm, *Brachychiton Populneus*

Dyes are widely used in many industries such as paper, cosmetics, leather, food, but especially in the textile industries to color their final product and which consume substantial volumes of water[1,2]. The presence of dyes in the aquatic environment has been a big issue for scientists due to their chemical structure. Such dyes can be classified as anionic, cationic and non-ionic; dyes are non-biodegradable and resistant to heat, light, many chemicals and oxidizing agents. Therefore, synthetic dyes disposal has resulted in serious health problems and the aquatic environment because of the mutagenic, carcinogenic, or toxic properties of the dyes and their potential to contaminate water resources[3]. To deal with this problem, industrial effluents must be treated prior to disposal.

Various techniques available for the treatment of wastewater containing dyes can be used. These include membrane filtration, in particular nanofiltration and reverse osmosis[4]; adsorption on activated carbon, especially in the case of Cationic dyes[5]; coagulation and flocculation[6]; advanced oxidation processes (POA)[7] and biological treatments[8]. Among these methods of treatment, adsorption remains one of the most promising techniques because of its convenience, simplicity of use and inexpensive nature compared to other methods[9]. The increasing demand for the adsorbents used in these processes has made their price higher and higher. This leads to further research in the manufacture of new, and less expensive adsorbent from materials that are conventional; specifically from waste vegetables, namely: sawdust[10], olive kernels[11], or fruit shells[12,13]. These adsorbents are natural materials available in large quantities at lower cost.

In the present work, *BrachychitonPopulneus* fruit shell has been employed for the preparation of activated carbon, and its effectiveness in the removal of the cationic dye, Methyl Green (MG), in aqueous phase by adsorption has been studied.Prepared carbon was characterized by several techniques: FTIR, SEM and BET. The factors influencing the adsorption, such as the initial concentration of the MG, the adsorbent dose and the temperature have been investigated. Furthermore, the kinetic, isotherm and thermo-dynamic parameters were evaluated in order to determine the efficiency of the adsorbent during the adsorption process.

Experimental Section

Adsorbate

The dye considered in this study is methyl green (MG), very high purity (99%), chemical formula $C_{26}H_{33}Cl_2N_3$, molecular weight = 458.47 g/mol, λ_{max} = 632 nm, was provided by Sigma-Aldrich. The stock

solution (100 mg/L) was prepared by dissolving some methyl green (0.1 g) in distilled water (1 L). Serial dilutions were made by diluting in with double distilled water.

Preparation of activated carbon

Figure 1 shows the *BrachychitonPopulneus* fruit shell collected from the region of Jijel (East of Algeria) which becomes an agricultural waste after it fall. The collected shells were extensively washed with distilled water and air-dried. Air dried shells were ground in a mortar into fine powder. Chemical activation by NaOH (5M) for 5 h was performed in controlled atmosphere (flowrate 0.330 L/min of vapor water) and held at that temperature 600°C for 1 h. The activated shell was washed first with a solution of HCl (0.1M) and later with hot distilled water until completely depleted of chloride ions. The obtained activated carbon (AC) crushed and sieved in order to have particles of the same size (<125 nm) and stored in airtight boxes.

Characterization

Fourier Transform Infrared (FTIR) analysis was applied to identify the characteristic functional groups, by using an FTIR spectroscope (FTIR- 8400 S Shimadzu). The spectra were recorded from 4000 to 400 cm^{-1} and the samples were prepared as pellets from a mixture of 3 mg of the sample with 300 mg of KBr under high pressure.

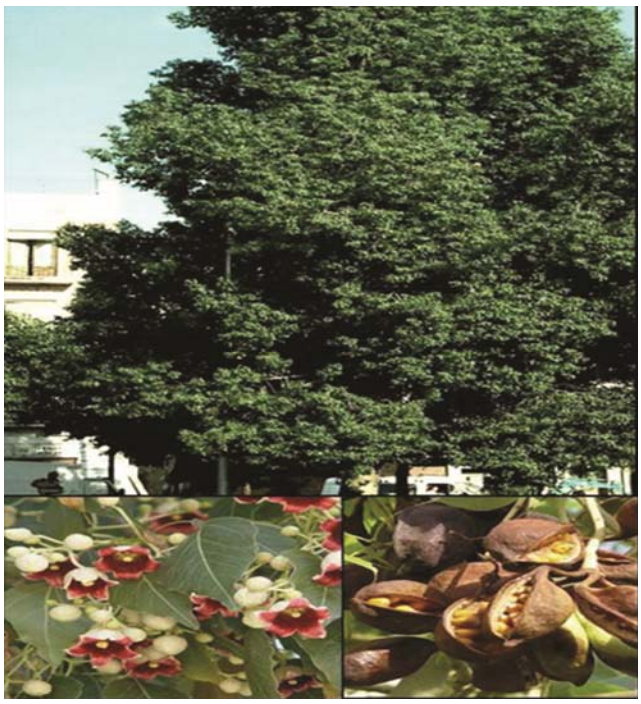

Fig. 1 — Image of *BrachychitonPopulneus* fruit shell.

The determination of point of zero charge of activated carbon was performed using the method reported by Boukhemkhem*et al.*[14]. For this purpose, 25 mL of a 0.01 M sodium chloride (NaCl) solution was placed in 50 mL erlenmyer flask. The *p*H was then adjusted to successive initial values between 2 and 12, by using either sodium hydroxide or hydrogen chloride (0.1N), and 0.1 g of adsorbents were added to the solution. After a contact time of 24 h, the final *p*H was measured and plotted against the initial *p*H. The pH_{PZC}value of the adsorbent can be determined at the point of intersection of the curve to X-axis.

Textural characterization of the activated carbon was done by using N_2 adsorption–desorption at 77K in a Micromeritics ASAP2010 apparatus. Prior to the measurements, the samples were outgassed at 180°C under nitrogen for at least 2 h. The specific surface area and pore size distribution were respectively determined by BET and BJH methods.

The morphology of the adsorbent was observed by SEM using a PHILIPS XL 30 ESEM apparatus.

Experimental adsorption procedure

The tests of the adsorption kinetics were carried out in a batch reactor, by stirring the colored synthetic solution of MG in the presence of a fixed amount of adsorbent (1g/L) at constant temperature. Samples of 1.0 mL were collected at regular time intervals, centrifuged and analyzed. The effect of initial MG dye concentration (20, 50 and 80 mg/L), adsorbent dose (25- 150 mg of AC) and temperature (20, 30 and 40°C) were evaluated in an experiment by varying those parameters, while keeping the others. The adsorption isotherms were established at room temperature with a solid/liquid ratio of 5 g/L using suspensions with increasing MG concentrations (20-200 mg/L). The suspensions were stirred for 2-3 h, thereafter there was no significant change in the concentration of MG at equilibrium.

The concentration of MG in the solutions before and after kinetic /equilibrium were determined by UV-visible spectrophotometer (UV-1601Shimadzu) at the wavelength which corresponds to the maximum absorbance of the MG (λ_{max} = 662 nm). All the experiments have been performed in triplicate and the mean values were reported.The amount of adsorption at t time ($q_t$mg/g), equilibrium ($q_e$mg/g) and adsorption efficiency (R%) were calculated according to the expressions:

$$q_t = \frac{(C_0 - C_t).V}{W} \quad \ldots (1)$$

$$q_e = \frac{(C_0 - C_e).V}{W} \quad \ldots (2)$$

$$R\% = \frac{(C_0 - C_e)}{C_0} \quad \ldots (3)$$

whereC_0, C_e and C_t(mg/L) are the concentrations of MG dye solution at respectively initial, equilibrium and at time (t). V (L) is the volume of the solution and W (g) is the mass of the used adsorbent.

Results and Discussion

Characterization of the adsorbent

The FTIR spectrum of the AC adsorbent is presented in Fig. 2. The broadbandbetween 3680-3100 cm^{-1} is typically ascribed to hydroxyl groups or adsorbed water[15]. Large peaks corresponding to the anti-symmetric stretching of CO_2 appear at 2360. The band around 1593 cm^{-1} is usually caused by the elongation vibrations of C = C groups of olefins (alkenes) and aromatics[16]. A low band near 1364 cm^{-1}indicated the deformation vibrations of the C-H group in the aliphatic chains[17]. A small band between 1000 and 1120 cm^{-1} characterize de formation of the aliphatic C-O groups. The bands around 991, 992, 865 and 730 cm^{-1} were assigned to the deformation vibrations of aromatics C-H[16,18]. This characterization reveals that several functional groups are present on the adsorbent, which are responsible for the binding of cationic dye MG.

The specific surface area and the pore size of an adsorbent are very important for the adsorption of dye since a higher surface area possesses more active sites. The adsorption–desorption isotherm of activated carbon (Fig. 3a) is a type IV isotherm, characterized by mesoporous adsorbent. A hysteresis type H3 loop also appears, corresponding to pore as slots whose liquid nitrogen was condensed in slit-shaped mesopores[19]. The pore size distribution curve in the Fig. 3b shows most mesoporous structures between 5 and 30 nm with the average pore diameter of 12.5 nm. The S_{BET} surface area of activated carbon was 656 $m^2.g^{-1}$ and total obtained pore volume was 0.369 $cm^3.g^{-1}$. The large specific surface area and mesoporous structures would be beneficial to the adsorption of MG on this prepared activated carbon.

The SEM images of the activated carbon prepared are shown in Fig. 4. Heterogeneous pores were clearly observed on the surface of the activated carbon and were organized by a group of honeycombed structures[20]. This might be due to the used activation process, involving both chemical and physical activating agents. Moreover, the presence of these open cylindrical and heterogeneous pores are at the origin of the large specific surface area from 656 m^2/g[21,22].

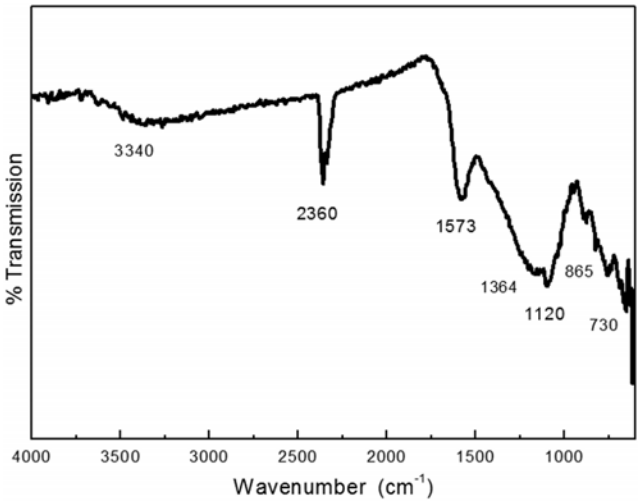

Fig. 2 — IR spectra of activated carbon.

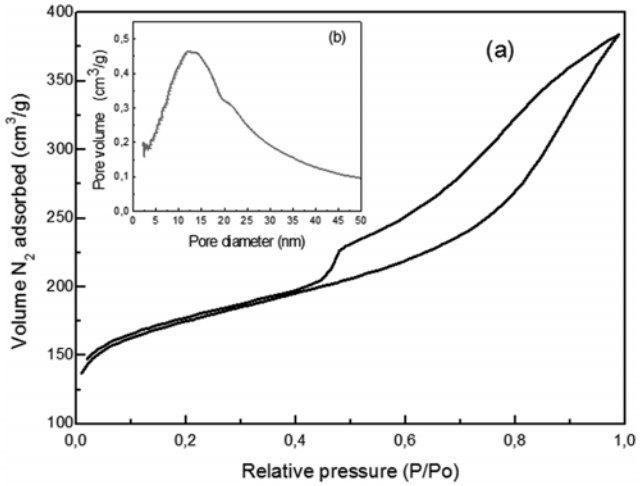

Fig. 3 — N_2 adsorption isotherm of activated carbon (a) and Pore size distribution of activated carbon (b).

Effect of various parameters on dye removal

Effect of initial concentration and contact time

Figure 5 shows the adsorption of MG onto activated carbon at different contact times for three initial concentrations of the dye. The data depicted in this Fig show that the percentage removal of MG for all three concentrations of dye increased gradually until equilibrium was attained. The higher adsorption rate during the initial period may be due to the high number of available adsorption sites. However, after this stage, the number of sites available of adsorption

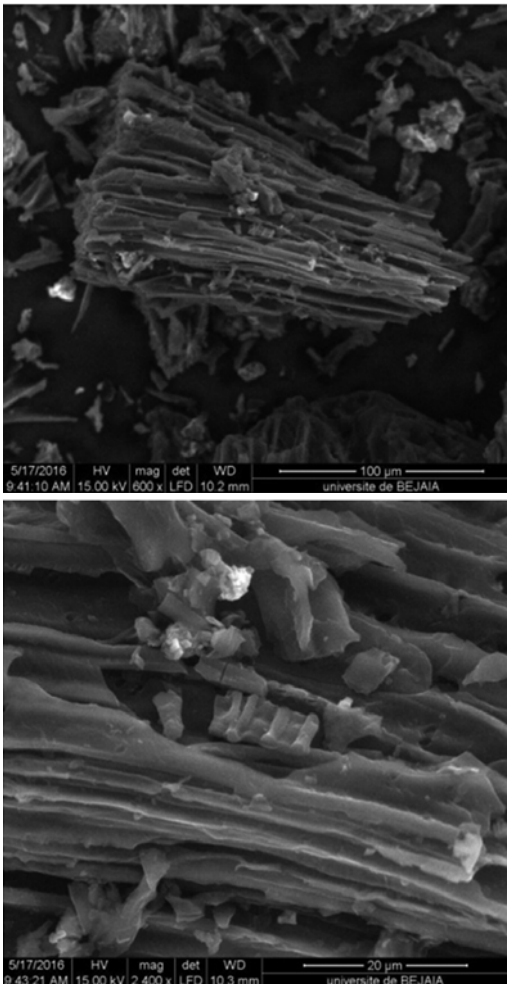

Fig. 4 — SEM images of activated carbon.

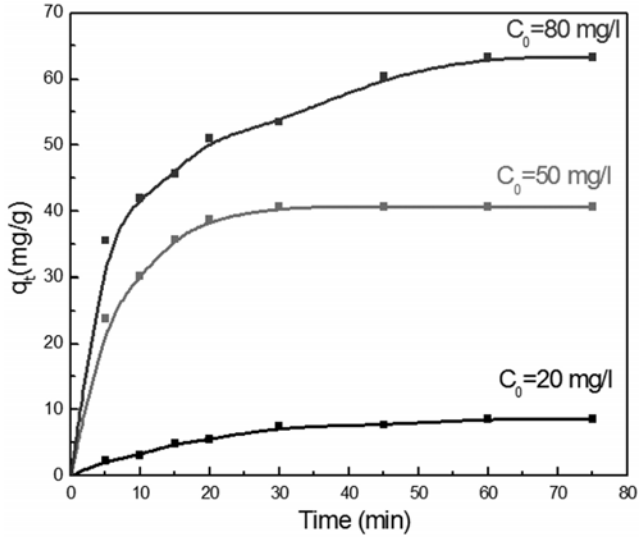

Fig. 5 — Effect of contact time and initial concentration of MG on the adsorption.

diminished as the dye molecules required longer time period to reach the least accessible sites. Furthermore, the quantity of dye removed increased from 8.66 to 63.38 mg/g, along with initial dye concentration of 20 to 80 mg/L. Similar results have been reported in the literature for dye removal by other adsorbents[23-26].

Effect of the amount of adsorbent

The effect of adsorbent dosage on MG adsorption was studied employing different masses of AC adsorbent (ranging from 25 to 150 mg), an initial MG ion concentration of 50 mg/L and an initial *p*H solution of the solution. As shown by the data depicted in Fig. 6a, the percentage removal of MG dye by AC increased initially with increasing adsorbent dosage and then became constant. The removal efficiencies of dye increased when the amount of AC increased, since the number of the active sites to which the dye molecules could bind increased[25,27]. The optimal adsorbent concentrations were found to be 6 g/L which was sufficient to achieve 78% removal of MG by AC.

Effect of agitation speed

The effect of stirring speed on the removal of MG on AC was investigated at different stirring speeds. Figure 6b shows that adsorption of MG increases with stirring speed, and maximum adsorption occurred at 600 rpm. Increasing agitation speed decreases the boundary layer resistance of the transfer of adsorbate molecules from the bulk solution to the adsorbent surface[28].

Effect of pH solution

One of the more important factors affecting the removal of dyes is the *p*H solution. This parameter affects not only the adsorption capacity, but also the

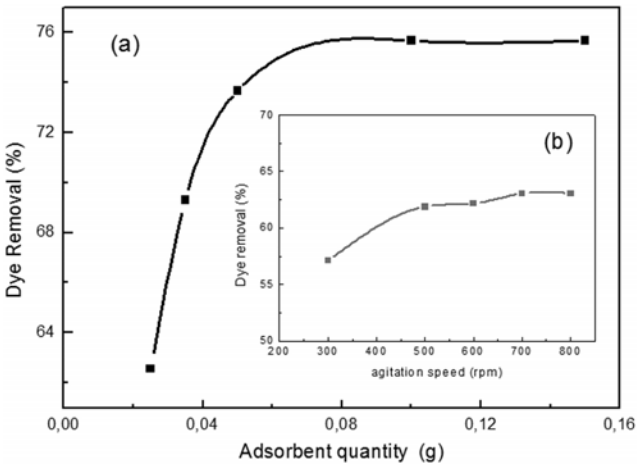

Fig. 6 — Effect of adsorbent dose on removal efficiency (a) and effect of agitation speed (b).

color of the dye solution and the solubility of some dyes[29]. The effect of initial *p*H of dye solution on the removal percentage of MG was studied by varying theinitial*p*H from 2 to 10 under constant process parameters(Fig. 7a). A significant increase in the removal efficiency was observed over the *p*H range of 2− 8.6 and remained constant thereafter. The variation in the removal of MG with respect to *p*H can be explained by considering the surface charge of activated carbon. For this, the pH_{PZC} measurement of AC was determined and shown in Fig. 7b. Therefore, we can say that at *p*H <pH_{pzc}= 8.76, the carbon surface has a net positive charge, and the dye becomes protonated when the electrostatic repulsion increases. Thus, the adsorption rate is decreased in the lower *p*H. When the *p*H is increased, the electrostatic attraction increased and the dye removal increased[30].

Modeling of adsorption kinetics

The mechanisms of adsorption involve a number of interactions or physico-chemical phenomena to explain what happens at the interface between the adsorbent, the pollutant and the aqueous solution[31, 32]. In order to describe the mechanism of adsorption kinetics, the linear forms of the pseudo-first-order[33], the pseudo-second-order[34] and intraparticle diffusion[35] kinetics models were employed to test the experimental data for MG dye adsorption onto activated carbon (AC).

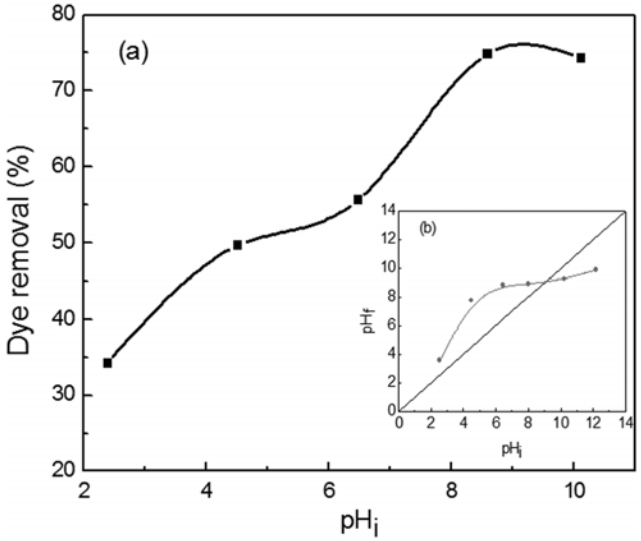

Fig. 7 — Effect of initial *p*H on removal efficiency (a) and the pH_{ZCN} of AC (b).

$$\ln(q_e - q_t) = \ln q_e - k_1 t \quad \ldots (4)$$

$$\frac{t}{q_t} = \frac{1}{k_2 q_e^2} + \frac{1}{q_e} t \quad \ldots (5)$$

$$q_t = k_{id}.t^{0.5} + C_{id} \quad \ldots (6)$$

whereq_e and q_t(mg.g^{-1}) respectively indicate the adsorption capacities at equilibrium and att time (min); k_1 (min^{-1}) is the pseudo-first-order rate constant; and k_2 (gmg^{-1}min^{-1}) is the rate constant of pseudo-second-order, k_{id} (g.mg^{-1}.min$^{1/2}$) is the intra-particle diffusion rate constant and C_{id} is the intercept which reflects the boundary layer effect.

In most cases, the pseudo-first-order equation of Lagergren does not fit well for the whole range of contact time and is generally applicable over the initial stage of the adsorption process[36]. However, over a long period the pseudo-second-order kinetic model provides the best correlation for all of the systems studied[34].

The kinetic parameters of the three models and the values of the corresponding linear regression correlation coefficients are listed in Table 1. It is obvious from Table 1 that the correlation coefficient R^2 of pseudo-first-order kinetics ranged from 0.89 to 0.97 and the calculated q_e (mg/g) values obtained from pseudo-first order kinetics did not well correspond with the experimental q_e (mg/g) values. Thus, it can be concluded that it is not appropriate to use the pseudo-first-order kinetic model to predict the adsorption kinetics for MG dye onto AC. The linear form of the plot of t/q_t versus t depicted in Fig. 8 and the highest correlation coefficient (R^2 = 0.99) listed in Table 1 clearly indicate that the adsorption kinetics of MG from aqueous solutions onto AC were well fitted by the pseudo-second-order model. This is also confirmed by the ($q_{e,exp}$) experimental value and the($q_{e,cal}$) calculated value which are quite close to

Table 1 — Kinetic parameters for adsorption of methyl green on AC

C_0 (mg/l)	$q_{e,exp}$ (mg/g)	Pseudo-first-order			Pseudo-second-order			Intraparticle diffusion		
		k_1 (min^{-1})	$q_{e,cal}$ (mg/g)	R^2	k_2 (g.mg^{-1}.min^{-1})	$q_{e,cal}$ (mg/g)	R^2	k_{id} (g.mg^{1}.min$^{1/2}$)	C_{id} (mg/g)	R^2
20	8.66	0.053	11.08	0.8898	0.004	8.41	0.9968	1.00	0.00	1.00
50	40.61	0.146	39.88	0.9746	0.007	42.85	0.9965	6.781	8.82	0.9848
80	63.38	0.060	45.83	0.8896	0.002	69.16	0.9943	6.730	20.44	0.9807

each other, as shown in Table 1.Similar phenomena have been observed in the adsorption of MG onto various adsorbent[24,25,37].

Linear plot of q_t versus $t^{0.5}$is shown in Fig. 9 for the three concentration dyes and the kinetic parameters are listed in Table 1. If the regression of q_t versus $t^{0.5}$ is linear and passes through the origin, then intra-particle diffusion is regarded only as the rate controlling step. If the plot shows multi-linearity, this suggests that adsorption involves intra-particle diffusion, that is governed by film diffusion. The intraparticle diffusion plots should be divided into two linear sections. The first linear plot represents gradual diffusion of dyes to adsorption site i.e. pore diffusion. After this time, we noticed that the systems had reached the equilibrium state. Similar behaviourwas reported for biosorption of basic dye[38]. As seen from Fig. 9, the plots were not linear over the whole time range. This indicates that the intraparticle diffusion was involved in the adsorption process, but was not the only rate controlling step[39,40].

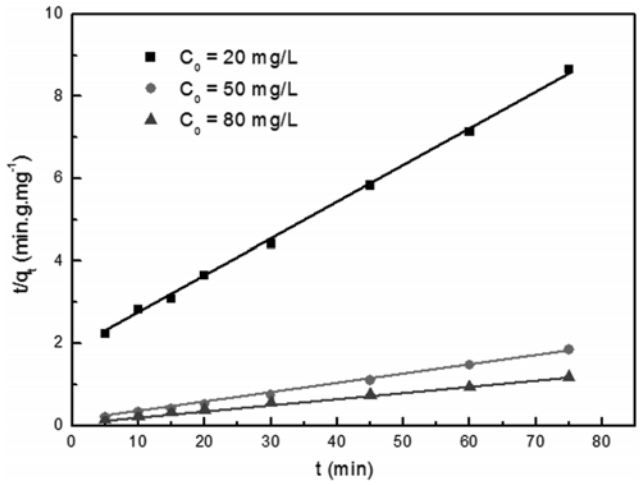

Fig. 8 — Pseudo-second-order kinetic plots for the adsorption of MG on AC.

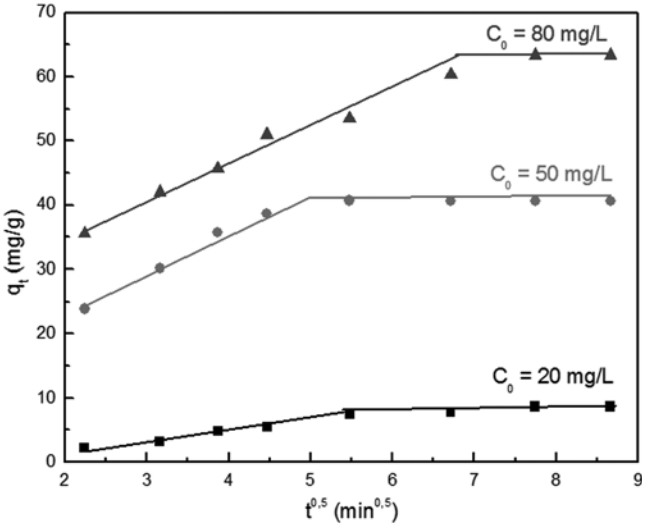

Fig. 9 — Intraparticle diffusion kinetic model for the adsorption of MG on AC.

Thermodynamics studies

Effect of temperature

The uptake of MG by AC was studied in 20, 30 and 40°C. A modest increase of the dye removal by AC can be seen from the Fig. 10a. This goes from 42% to 54%, indicates the endothermic nature of this adsorption process. Many authors related their results to the fact that higher temperatures mean higher activities for mobile ions and thus higher rates of contact between these ions and adsorbing surfaces[23,41].

Thermodynamic parameters

The thermodynamic parameters of the adsorption process of MG on the AC, such as the enthalpy ΔH°, the entropy ΔS° and the free enthalpy ΔG° have been determined inthe following equations [37]:

$$\Delta G^o = -RT\ln(K_d) \quad \ldots (7)$$

$$\ln(K_d) = -\frac{\Delta H^o}{RT} + \frac{\Delta S^o}{R} \quad \ldots (8)$$

where R is a universal gas constant (8.314 J/mol.K) and $K_d = q_e/C_e$ is the equilibrium partition constant.

Van't Hoff plot of $\ln(K_d)$ vs 1/T is shown in Fig. 10b and Table 2 summarized the thermodynamic parameters determined at different temperatures range

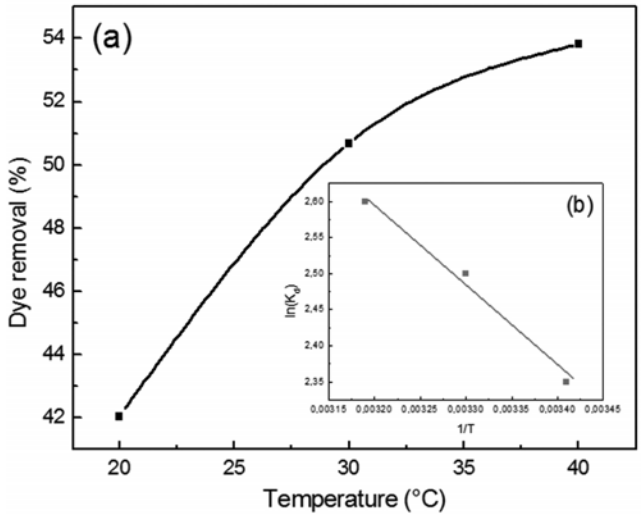

Fig. 10 — Effect of temperature on removal efficiency (a) and Van't Hoff plot of $\ln(K_d)$ vs 1/T (b).

Table 2 — Thermodynamic parameters for the adsorption of MG dye on AC

T (K)	ΔG^0 (kj/mol)	ΔH^0 (kj/mol)	ΔS^0 (j/mol.K)
293	-14.33		
303	-15.44	18.14	110.82
313	-16.55		

from 293 K to 313 K. It can be seen that the negative values of ΔG° indicate the spontaneous nature of the adsorption. The positive values of ΔH suggest the endothermic nature of the adsorption interaction, and its low value (<40 kJ.mol^{-1}) indicates that it is a physisorption. The positive value of ΔS° show the increasing randomness at the adsorbent/solution interface during the adsorption process[42].

Modeling of adsorption isotherms

The adsorption isotherm data (Fig. 11) revealed that theamount of dye adsorbed increased with increasing equilibrium concentration of dyes. The isotherm showed the shape of type "S" according to the classification of Giles *et al.*[43]. The "S" shape of the isotherms means that a cooperative adsorption, in which the adsorbate-adsorbate interaction is stronger than that between adsorbent and adsorbate.

In order to identify the retention mechanism and identify the isotherm, which better represents the dye adsorption studied on AC, three theoretical models were tested on the obtained experimental data, namely Langmuir[44], Freundlich[45] and Redlich – Peterson[46]. These isotherm models are represented by the following respective equations:

$$q_e = \frac{q_m K_L C_e}{1 + K_L C_e} \quad \ldots (9)$$

Where q_m is the maximum adsorption capacity (mg/g) and $K_L$is the Langmuir constant (L/mg).

$$q_e = K_F C_e^{1/n_F} \quad \ldots (10)$$

Where K_F [(mg/g)(L/mg)$^{1/n_F}$] and $\boldsymbol{n_F}$ (dimensionless) are the characteristic Freundlich constants

$$q_e = \frac{q_{RP} K_{RP} C_e}{1 + K_{RP} C_e^{\alpha}} \quad \ldots (11)$$

whereq_{RP}, K_{RP} and α are the characteristic Redlich - Peterson constants

Table 3 — Isotherm parameters and correlation coefficients for the adsorption of methyl green on AC

Isotherm models	Correlation parameter Name	Value	Correlation coefficient R^2
Langmuir	q_m (mgg^{-1})	67.93	0.9853
	K_L(Lmg^{-1})	0.06	
Freundlich	K_F(L mg^{-1})	8.51	0.7626
	n_F	0.427	
Redlich-Peterson	q_{RP}(mg g^{-1})	59.33	0.9811
	K_{RP}(Lg^{-1})	0.08	
	α	0.95	

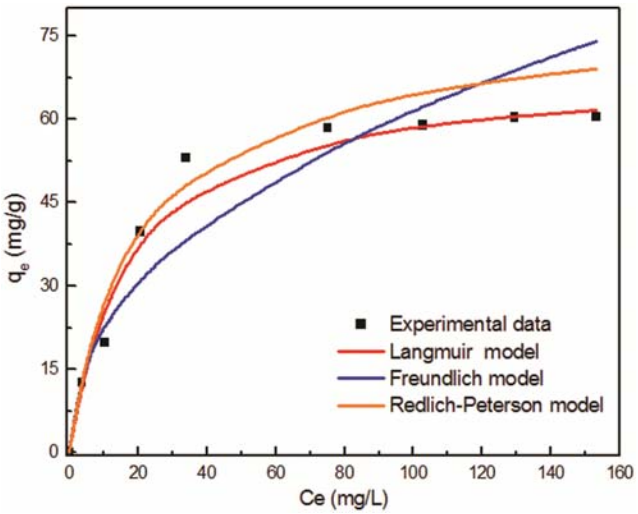

Fig. 11 — Equilibrium isotherm of MG on activated carbon.

The experimental adsorption data for MG on AC has been analyzed by Langmuir, Freundlich and Redlich-Peterson isotherms in non linear form which have been shown in Fig. 11. The adsorption constants and the correlation factors for all the isotherms evaluated are listed in Table 3. The correlation coefficient R^2 values indicate that the Langmuir and Redlich-Peterson isotherms models better describe the MG adsorption on AC than found for Freundlich. The maximum adsorption capacity obtained using the Langmuir isotherm is 67.93 mg g^{-1} and the langmuir isotherm indicates that the adsorption of MG onto AC was a monolayer adsorption trend. The value of n_F for MG lied between 0 and 1 further confirming the favorable adsorption for MG dye.

The maximum adsorption capacity (q_m) of AC for MG was compared with those reported in the literature for different adsorbents and shown in Table 4. It could be concluded that AC has a relatively higher adsorption capacity than the other kinds of adsorbents. These results point out that activated

Table 4 — Comparison of adsorption capacity of MG by various adsorbents

Adsorbent	q_m (mg/g)	Reference
Activated carbon (AC)	67.93	In this work
Zeolite H-ZSM-5	70.08	[23]
Carbon nanotubes (CNT)	146	[25]
Carbonnanotubes(CNT-$NiFe_2O_4$)	88.50	[25]
Bamboo	20.41	[26]
Loofah fiber	18.16	[41]
Activated carbon (Seed Shells)	58.82	[47]

carbon prepared from *BrachychitonPopulneus* fruit shell could be employed as a promising adsorbent for the removal of cationic dye methyl green from aqueous solutions.

Conclusion

The present study aims to develop an adsorbent from agricultural waste to remove cationic MG dye from aqueous solution. The characterization results showed that prepared activated carbon reveals several functional groups and high BET surface areas (660 m^2/g). Similarly, the MG dye adsorption capacity also increased with increasing contact time and adsorbent dosage.Adsorption processes for MG dye on AC were found to follow the pseudo second-order kinetics rate expression. The equilibrium data were well fitted by the Langmuir and Redlich-Peterson adsorption model with a maximum equilibrium adsorption capacity of 67.93 mg / g for MG. As well, the values of the thermodynamic parameters characterized the adsorption as an exothermic and spontaneous physisorption.

All these results reveal that active carbon synthesized (AC) from the natural fruit shell waste could be effectively used as a low cost adsorbent for the removal of the green methyl dye from an aqueous solution.

Acknowledgements

The authors would like to thank the Ministèrede l'Enseignement Supérieuret de la Recherche Scientifiquein Algeria and the Research Laboratory (LIME) of the University of Jijel for their technical and financial assistance.

References

1 Bendi R, Pathpireddy M K R &Challapalli S, *Energy*, 33 (2014) 38.
2 Saucier C, Adebayo M A, Lima E C, Prola L D T, Thue P S, Umpierres C S, Puchana-Rosero M J & Machado F M, *Clean – Soil Air Water*, 43 (2015) 1389.
3 Almeida E J R & Corso C R,*Chemosphere*, 112 (2014) 317.
4 Khettaf S, Bouhidel K E, Meguellati N H, Ghodbane N H & Bouhelassa M, *Water Envi J*,30 (2016) 179.
5 Seow T W & Lim C K, *Int J ApplEng Res*, 11 (2016) 2675.
6 Verma A K, Dash R R&Bhunia P, *J EnviManag*, 93 (2012) 154.
7 Hassaan M A& El Nemr A, *Int J PhotochemPhotobio*, 2 (2017) 85.
8 Archna K N, Lokesh R R& Siva K, *J Biochem Tech*, 3 (2012) 177.
9 Mohammed M A, Shitu A & Ibrahim A, *Res J ChemSci*, 4 (2014) 91.
10 Srinivasakannan C &Balasubramaniam N, *J Part Sci Tech*, 25 (2007) 535.
11 Hazza R & Hussein M, *Envi Tech Innov*,4 (2015) 36.
12 Tongpoothorn W, Sriuttha M, Homchan P, Chanthai S &Ruangviriyachai C, *ChemEng Res Design*,89 (2011) 335.
13 Gottipati R & Mishra S, *Can J ChemEng*,91 (2013) 1215.
14 Boukhemkhem A & Rida K, *AdsorSci Tech*, 35 (2017) 753.
15 Dhawane SH, Kumar T &Halder G, *Energy Convers Manage*,100 (2015) 277.
16 Petrov N, Budinova T, Razvigorova M, Ekinci E, Yardim F &Minkova V, *Carbon* , 38 (2000) 2069.
17 Das D, Samal D P &Meikap B C, *J ChemEng Process Technol*,6 (2015) 1.
18 Makeswari M &Santhi T, *J Water Res Prot*,5 (2013) 222.
19 Guedidi H, Reinert L, Lévêque J, Soneda Y, Bellakhal N & Duclaux L, *Carbon*,54 (2013) 432.
20 Intidhar JI, *AdsSci Tec*, (2017)1.
21 Thambiannan S, Rajendran R & Lima RM, *CLEAN – Soil Air Water*, 41 (2013) 797.
22 AhiduzzamanMd&SadrulIslam AKM, *Springer Plus*, 5 (2016) 1248.
23 Maaza L, Djafri F&Djafri A, *Orient J Chem*, 32 (2016) 171.
24 Bagane M &Guiza S, *Ann ChimSci Mat*, 25 (2000) 615.
25 Bahgat M, Farghali A A, El Rouby W, Khedr M &Mohassab-Ahmed Y, *ApplNanosc*, 3 (2013) 251.
26 Atshan A A, *Iraqi J Chem Petrol Eng*, 15 (2014) 65.
27 Rytwo G, Nir S, Crespin M & Margulies L, *J Coll Inter Sci*, 222 (2000) 12.
28 Zahoor M, *J ChemSocPak*,33 (2011) 305.
29 Fu Y &Viraraghavan T, *BioresourTechnol*,79 (2011) 251.
30 Baseri J R, Palanisamy P N & Kumar P S, *Indian J ChemTechnol*, 19 (2012) 311.
31 Dos Reis LGT, RobainaNF, Pacheco WF &Cassella R J, *ChemEng J*,171 (2011) 532.
32 SalhD M, *J Envi Earth Sc*i, 4 (2014) 50.
33 Singh V K & Tiwari P N, *JChemTechnolBiotechnol*, 69 (1997) 376.
34 Ho Y S & Mc Kay G, *Pro Bioch*,34 (1999) 451.
35 Weber W J & Morris J C, *J Sanitary Engg Div. American Soc Civil Eng*, 89 (1963) 31.
36 Ho Y S & Mc Kay G, *Trans I Chem E*,76 (1998) 332.
37 Sharma P, Saikia B K & Das M R, *Colloids Surf. A PhysicochemEng Asp,*457 (2014) 125.
38 Banerjee S, Sharma G C, Gautama R K, Chattopadhyaya M C, Upadhyay S N & Sharma YC, *J MolLiq*,213 (2016) 162.
39 Ofomaja A E &Unuabonah E I, *J Taiwan Inst ChemEng*, 44 (2013) 566.
40 Rida K, Bouanika A, Boudellal M &Boukhemkhem A, *Desali Water Treat*,56 (2015) 2731.

41 Tang X, Li Y, Chen R, Min F, Yang J & Dong Y, *Korean J Chem Eng*, 32 (2015) 125.
42 Chakraborty S, De S, Das Gupta S & Basu JK, *Chemosphere*, 58 (2005) 1079.
43 Giles C H, Smith D &Huitson A, *J Colloid Interf Sci*, 47 (1974) 755.
44 Langmuir I, *J Am ChemSoc*, 38 (1916) 2221.
45 Freundlich H M F, *J Phys Chem*, 57 (1906) 385.
46 Jossens L, Prausniz J M, Fritz W, Schlunder U & Myers A L, *Chem Eng Sci*, 33 (1978) 1097.
47 Chinenye AI, PiusC O, Okechukwu D O &IkennaC N, *World J EngTechnol*,(2016) 421.